

Z. GLAVAS*, F. UNKIĆ*, D. LISJAK**

THE PREDICTION OF THE MICROSTRUCTURE CONSTITUENTS OF SPHEROIDAL GRAPHITE CAST IRON BY USING THERMAL ANALYSIS AND ARTIFICIAL NEURAL NETWORKS

PRZEWIDYWANIE ELEMENTÓW MIKROSTRUKTURY SFEROIDALNEGO GRAFITOWEGO ŻELIWA Z ZASTOSOWANIEM ANALIZY TERMICZNEJ I SZTUCZNYCH SIECI NEURONOWYCH

This paper presents the application of artificial neural networks in the production process of spheroidal graphite cast iron. Backpropagation neural networks have been established to predict the microstructure constituents (ferrite content, pearlite content, nodule count and nodularity) of spheroidal graphite cast iron using the thermal analysis parameters as inputs. Generalization properties of the developed artificial neural networks are very good, which is confirmed by a very good accordance between the predicted and the targeted values of the microstructure constituents on a new data that was not included in the training data set.

Keywords: spheroidal graphite cast iron, microstructure constituents, thermal analysis, artificial neural networks

Praca przedstawia zastosowanie sieci sztucznych neuronów do procesu wytwarzania sferoidalnego żeliwa grafitowanego. Celem przewidzenia składowych mikrostruktury (składowej ferrytycznej, składowej perlitycznej, ilość grafitowych wtrąceń kulistych, kulistość wtrąceń) sferoidalnego żeliwa grafitowanego, ustalona została jako danych wejściowych.

Ogólne własności zbudowanej sieci neuronowej są bardzo dobre, co zostało potwierdzone poprzez bardzo dobrą zgodność przewidywanych i uzyskanych wartości składowych mikrostruktury.

1. Introduction

Spheroidal graphite cast iron (SGI), also known as ductile iron (DI), is an excellent example of a material where the mechanical properties are determined primarily by its microstructure. The microstructure of a typical commercial SGI, in the as-cast condition, consists of graphite nodules which are embedded in the metal matrix (Figure 1). The metal matrix is usually a mixture of ferrite and pearlite.

The ferrite (pearlite) content in the metal matrix of SGI depends on the chemical composition, the cooling rate during the solidification and the subsequent transformation in the solid state, as well as the volume fraction and the number of graphite nodules [1-5]. Silicon promotes ferrite, while the elements Cu, Sn, Sb, Mn, Cr etc. are pearlite promoters [5-7]. The influence of the cooling rate on the microstructure of SGI is quite complex, since it affects both graphite morphology and the ferrite/pearlite ratio. A higher cooling rate during the solidification will increase graphite nodule count and

nodularity. However, higher cooling rates in the eutectoid transformation range result in a higher pearlite content in the microstructure [1, 8, 9]. Nodule count has a significant influence on the ferrite/pearlite ratio [1, 10, 11]. The increase of the nodule count per unit volume (reducing of the average nodules size at constant graphite volume fraction) results in the decreasing of the diffusional paths of carbon during the eutectoid transformation which leads to a higher ferrite content in the microstructure of SGI for the same chemical composition and cooling rate.

It is obvious that there is a large number of factors which influence the microstructure of SGI. The chemical composition does not give the insight into the metallurgical state of the melt, i.e. the quality and the susceptibility of the melt for obtaining the required microstructure and mechanical properties. For example, the chemical composition of SGI does not give the information about the metallurgical state of melt which has a significant influence on the nodule count in the microstructure. The

* FACULTY OF METALLURGY, UNIVERSITY OF ZAGREB, ALEJA NARODNIH HEROJA 3, 44103 SISAK, CROATIA

** FACULTY OF MECHANICAL ENGINEERING AND NAVAL ARCHITECTURE, UNIVERSITY OF ZAGREB, IVANA LUCICA 5, 10002 ZAGREB, CROATIA

melt control method which gives the insight into the metallurgical state of the melt is thermal analysis (TA). In the foundries, thermal analysis is performed by the recording of the cooling curves. The cooling curve incorporates the solidification history of the particular sample for which the curve was recorded. Many attempts have been made to correlate the data from the cooling curve with the shape of graphite, microstructure and mechanical properties [12-14]. In this paper the data from the cooling curves are correlated with the microstructure of SGI (ferrite and pearlite content, nodule count and nodularity).

The on-line prediction of the microstructure of SGI is important for the control of the casting properties. In order to obtain reliable models for the prediction of the microstructure of SGI, it is necessary to use artificial neural networks (ANN) because the casting production process is a complex and a non-linear process, i.e. the chemical composition, the metallurgical state of the melt and the microstructure are not in a linear relationship. ANN are complex systems composed of simple elements (artificial neurons) operating in parallel [15]. Two or more neurons may be combined in a layer, and a particular network might contain one or more layers (the input layer, the output layer and hidden layers). The network function is determined by the connections between the elements. We can train (learn) ANN to perform a particular function by adjusting the values of the connections (weights) between the elements. The most important and the most widely used algorithm for the ANN training (learning) is backpropagation. Each input to a neuron is weighted with an appropriate weight. The sum of the weighted inputs and the bias form the input to the neuron transfer function. It is the function that maps

a neuron's (or layer's) net output to its actual output. The most popular transfer functions are linear, log sigmoid, hyperbolic tangent sigmoid etc.

Properly trained ANN are capable to map the input to the output patterns with a minimal error between the predicted and the measured output values. The testing of ANN follows after the training. It is performed by a new input data set which is not included in the input data set for the training of ANN.

The goal of present research was to establish ANN models for predicting of the microstructure of the commercial SGI using the data from the cooling curves as inputs.

2. Experimental

Examinations were performed in the commercial foundry in real industrial conditions. The base melt for the production of SGI was produced in an acid-lined cupola furnace. The melt was transferred to the net-frequent induction furnace where the homogenization and the correction of the chemical composition were carried out. After that, the melt was desulphurized in a ladle by the addition of CaC₂ and strongly mixed with nitrogen which was introduced through a porous plug located at the ladle bottom. After the desulphurization and the removing of slag the melt was poured into a channel-type induction holding furnace (receptor). The nodularizing treatment of the base melt was performed by the Flotret method. After the treatment and inoculation, a sample of the melt was taken for the estimation of the chemical composition and a Y-block was cast. The chemical composition of the examined SGI melts is given in Table 1.

TABLE 1

Chemical composition (wt. %) of the SGI melts used in the experiments

C	Si	Mn	P	S	Ni	Cr	Cu	Mo	Al	Sn	Mg
3.3	2.7	0.1	0.030	0.005	0.03	0.02	0.08	0.003	0.009	0.005	0.029
—	—	—	—	—	—	—	—	—	—	—	—
3.4	3.0	0.2	0.045	0.010	0.04	0.04	0.50	0.009	0.015	0.015	0.040

A Y-block was cast into the mould which had been produced by the Betaset® process. The dimensions and the form of the Y-block are specified according to the EN 1563. Thermal analysis was performed by the advanced thermal analysis system. Altogether, 150 melts have been made.

Test pieces for the metallographic examinations were machined from Y-blocks and prepared by the standard metallographic technique. The quantitative metal-

lographic examinations (the estimation of ferrite content, pearlite content, nodule count and nodularity) were performed by a light metallographic microscope with a digital camera and the image analysis system.

The software used to create the ANN which predict the microstructure constituents of SGI using the selected TA parameters as inputs is Neural Network Toolbox of MATLAB® 7.0.

3. Results and discussion

With the goal of achieving a higher accuracy, a separate neural network was established for each microstructure constituent, except for pearlite content because the metal matrix of the analyzed samples was consisted of ferrite and pearlite. Percent of the ferrite in the metal matrix + percent of the pearlite in the metal matrix were 100 % of the metal matrix. The input parameters for the ANN were thermal parameters from the cooling curves in the eutectic and the eutectoid range and thermal parameters from the first derivative of the cooling curves in the eutectic range. Only the relevant thermal parameters

were selected as inputs parameters of the ANN. They are: ϑ_L (liquidus temperature, °C), ϑ_{Elow} (the lowest eutectic temperature or temperature of eutectic undercooling, °C), ϑ_R (recalescence, °C), ϑ_S (solidus temperature, °C), GRF1 (Graphite Factor 1), GRF2 (Graphite Factor 2), $d/dt\vartheta_S$ (value of the first derivative at solidus temperature or the depth of the first derivative (negative peak) at the solidus, °C/s) and ϑ_{Eoid} (eutectoid temperature, °C). Figures 2a and 2b schematically show the selected input parameters of the ANN on the cooling curve in the eutectic range and on the first derivative of the cooling curve in the eutectic range, respectively.

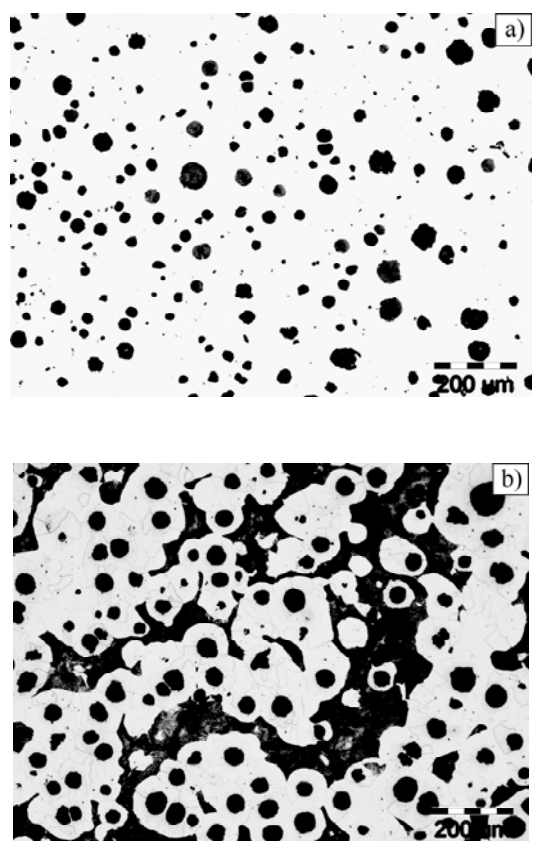


Fig. 1. Optical micrographs of a typical as-cast microstructure of spheroidal graphite cast iron: a) no etched; b) etched, nital

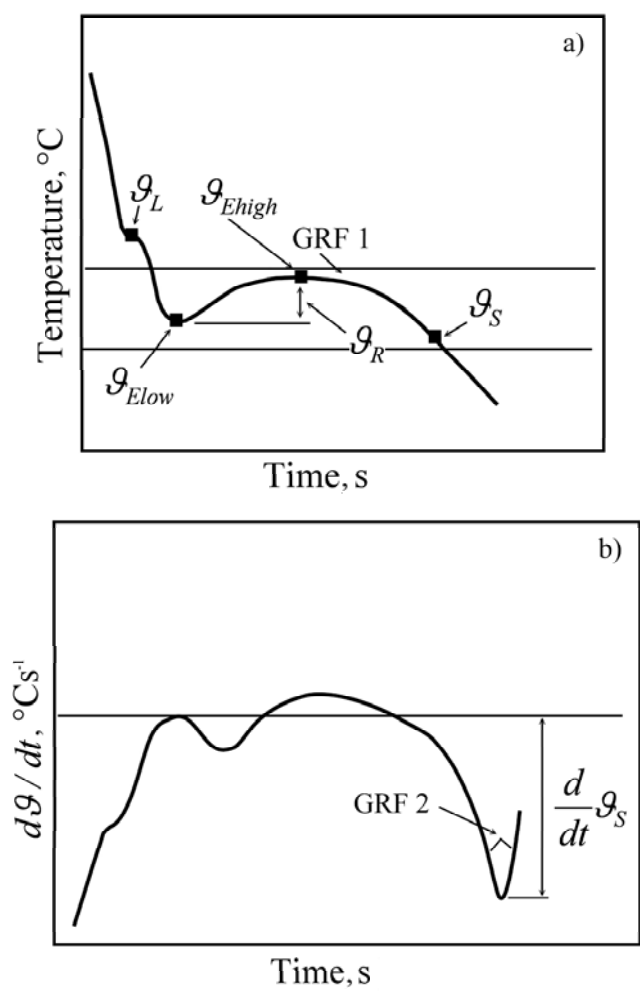


Fig. 2. a) Schematic description of the cooling curve of the SGI in the eutectic range with displayed TA parameters, b) Schematic description of the first derivative of the cooling curve in the eutectic range with displayed TA parameters

The eutectoid temperature (ϑ_{Eoid}) was not included as the input parameter of the ANN for the prediction of the nodule count and nodularity because the nucleation of new graphite particles during the eutectoid transformation is extremely difficult and the shape of graphite is established during the solidification and cannot be changed afterwards.

When creating a neural network, it is important to prevent the overfitting. In this work, the early stopping method was used to improve network generalization and prevent the overfitting. According to this method, the experimental data set is divided into three subsets: the training data set, the validation data set and the test data set. The training data set was used for computing the gradient and updating the networks weights and biases. Training was performed only on the training set. The validation data set was not included in the training data set and was used to decide when to stop the training. The test data set error was not used during the training, but it was used for the comparison of different models,

i.e. for the evaluation of the performance of networks. Network generalization is good when networks are able to perform as well on the test data set as on the training data set. To produce the most efficient training, the input and the output data are normalized before the training.

In this paper, different networks architectures were examined to determine the networks which have a minimum generalization error. The best results were achieved by the multilayer Backpropagation Neural Networks (BPNN) which are trained using the Levenberg-Marquardt algorithm. Optimum structure of network (number of layers, number of neurons, transfer functions etc.) was obtained using genetic algorithms (GA).

The performances of the trained BPNN were measured by the regression analysis between the networks outputs (predicted values) and the corresponding target values which had been obtained by measuring (Table 2). Figures 3a - 3c show the performances of the BPNN on the test data set.

TABLE 2

Values of coefficients correlation (R) on training, validation, test and entire data set

Coefficient correlation	Data set	BPNN1	BPNN2	BPNN3
R	Training data set	0.981	0.984	0.966
	Validation data set	0.958	0.951	0.907
	Test data set	0.966	0.950	0.772
	Entire data set	0.971	0.966	0.907

BPNN1 – the neural network to predict the ferrite content in the microstructure of SGI
BPNN2 – the neural network to predict the nodule count/mm² in the microstructure of SGI
BPNN3 – the neural network to predict graphite nodularity in the microstructure of SGI

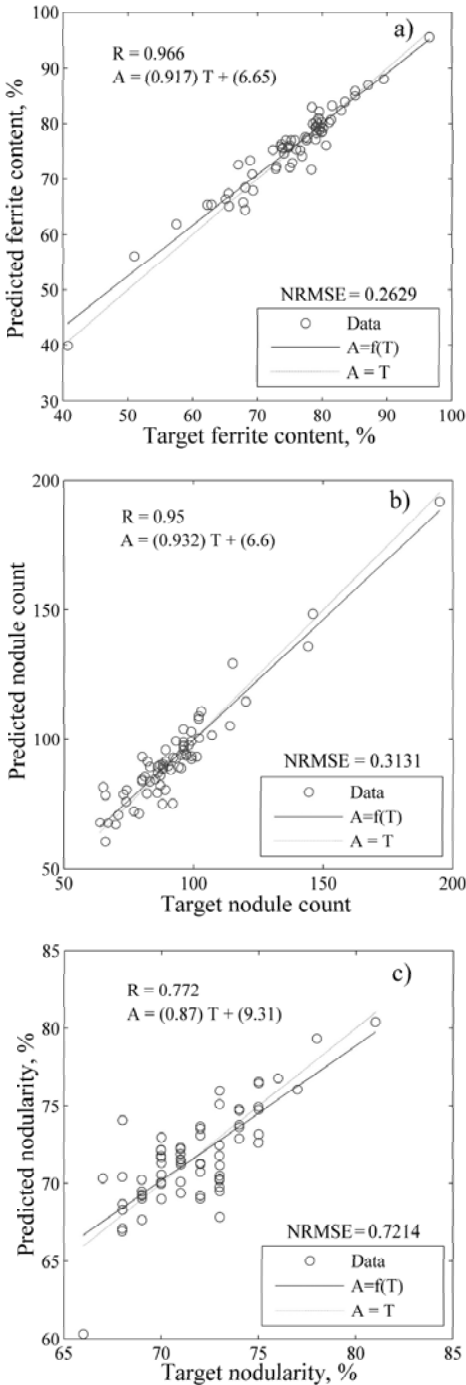


Fig. 3. a) Performance of the BPNN1 to predict the ferrite content on

the test data set, b) Performance of the BPNN2 to predict the nodule count/mm² on the test data set, c) Performance of the BPNN3 to predict nodularity on the test data set, R – coefficient correlation, A – predicted values, T – target values

Performance functions are important measures for the evaluation of a network’s performance. In this paper, the performance functions used for the training of BPNN are the Sum Squared Error (SSE), the Mean Square Error (MSE), the Root Mean Square Error (RMSE) and the Normalized Root Mean Square Error (NRMSE).

Figures 3a - 3c show a very good networks generalization which is confirmed by high values of coefficients correlation between the networks outputs and the corresponding target values obtained by measuring. This is the indication of proper networks architectures and proper selection of input networks parameters.

The obtained results show that the combination of thermal analysis and neural networks is a powerful tool for the prediction of the microstructure of SGI. Successfulness of the models is confirmed by high values of coefficients correlation between the measured and the predicted microstructure on the test data set.

Thermal parameters, which were taken as input variables for the neural networks, are closely connected with the chemical composition and the microstructure development of SGI. In the succession of discussion, there will be considered the influence of the selected TA parameters on the microstructure of SGI.

The liquidus temperature ϑ_L (Figure 2a) is closely related to the carbon equivalent (CE), i.e. with C and Si contents. Low values of the liquidus temperature are primarily the indication of high C contents. The combination of high C contents, i.e. carbon equivalent and slow cooling rates (thick sections), results in the flotation and formation of non-spheroidal graphite forms. The increasing of C contents may result in the increase of nodules count per unit volume and the decrease of the average distance between them. Silicon promotes ferrite. At very high contents, Si strengthens the ferrite, which has the influence on the mechanical properties of SGI.

The liquidus temperature ϑ_L , the temperature of the

start of the eutectic reaction ES and the lowest eutectic temperature ϑ_{Elow} of the examined melts are almost the same temperatures, which indicates the nearness of the eutectic composition and equal precipitation of the eutectic during the solidification, i.e. a continuous nucleation of graphite. The continuous nucleation of graphite during the solidification results in a higher density of graphite particles (high nodule count) in the metal matrix. During the eutectoid transformation, i.e. austenite decomposition, a high density of graphite particles acts on the decreasing of diffusional paths of C in the solid state, which results in the increasing of the ferrite content in the microstructure. Nodule count has a significant influence on nodularity. The increase of nodule count results in a decrease of their size and increase of nodularity.

The lowest eutectic temperature or the temperature of eutectic undercooling ϑ_{Elow} (Figure 2a) is related to the nucleation state of the melt. Low temperature of eutectic undercooling indicates poor nucleation properties of the melt i.e. a low number of active sites for the nucleation of graphite. A low number of active sites for the nucleation of graphite results in a low nodule count. Moreover, if the temperature of eutectic undercooling lies below the metastable temperature, primary carbides may occur in the microstructure.

Recalescence ϑ_{R} (Figure 2a) represents the difference between the highest eutectic temperature ϑ_{high} and the lowest eutectic temperature (the temperature of eutectic undercooling) ϑ_{Elow} . Recalescence is the indicator of eutectic growth, i.e. the amount of austenite and graphite precipitated during the early stage of eutectic solidification. High recalescence indicates poor nucleation susceptibility of the melt. Moreover, high value of recalescence is related to the non-continuous precipitation of graphite during the solidification. A too high amount of graphite precipitated in the early stage of eutectic solidification results in a small amount of graphite precipitated during the later solidification. Due to that, secondary sites of nucleations are not activated, which may result in a low nodule count.

The solidus temperature ϑ_{S} (Figure 2a) is an important thermal parameter for monitoring the end of the solidification. The segregation of carbide forming elements such as Cr, Mn, V etc. at cell boundaries causes an increase of the metastable eutectic temperature. If the solidus temperature lies below the metastable eutectic temperature, intercellular carbides may occur in the microstructure.

GRF1 (Figure 2a) is a parameter that reflects how much eutectic, i.e. eutectic graphite is precipitated from ϑ_{high} to ϑ_{S} . This parameter is defined as the relative time for the temperature to drop 15°C from the highest eutec-

tic temperature (ϑ_{high}). A high GRF1 indicates a continuous precipitation of eutectic graphite, which is related to the activation of secondary nucleation sites. This results in the moving of the eutectic reaction toward longer times. This mode of eutectic solidification, when the nucleation and the growth of eutectic occur in longer times, results in a higher distribution of sizes of the precipitated graphite, i.e. a higher density of graphite particles in the metal matrix. A higher number of graphite particles during the eutectoid transformation enable the formation of a higher ferrite content in the microstructure.

GRF2 (Figure 2b) is a parameter that reflects the change of the cooling rate at the end of the solidification, measuring indirectly thermal conductivity. The angle of the first derivative at the solidus temperature (ϑ_{S}) and the negative peak at the latest segment of the first derivative are used to calculate GRF2. Low value of GRF2 indicates high thermal conductivity, which is an indicator of a high amount of graphite at the end of the solidification. Low value of the first derivative of the cooling curve at the solidus (higher depth of the negative peak) $d/dt\vartheta_{\text{S}}$ (Figure 2b) is related to a high amount of eutectic graphite at the end of the solidification, i.e. a high nodule count in the SGI. Therefore, GRF2 combined with $d/dt\vartheta_{\text{S}}$ is a strong indicator of thermal conductivity, i.e. the graphite shape and nodule count in SGI.

The solid state transformation of austenite (γ) into ferrite (α) and graphite or pearlite ($\alpha + \text{Fe}_3\text{C}$) occurs in the eutectoid transformation range. The eutectoid transformation has an important influence on the final microstructure of SGI. The ferrite and pearlite content in the microstructure of SGI depends on the chemical composition, the cooling rate through the eutectoid transformation range and the volume fraction and the number of graphite nodules. When pearlite is created latent heat is released, which is visible as an arrest in the cooling curve. At higher amounts of pearlite, recalescence occurs during the eutectoid transformation. A fully ferritic SGI does not show recalescence. It has also been found that the increasing of the amounts of pearlite in the metal matrix lowers the eutectoid temperature. Therefore, the eutectoid temperature is the indicator of pearlite content in the metal matrix of SGI.

4. Conclusions

The obtained results show that the analysis of the cooling curves and neural network modeling enable the formation of mathematical models for the prediction of the microstructure constituents of spheroidal graphite cast iron before pouring of the melt into the moulds. The developed backpropagation neural networks successfully

predict the microstructure constituents using the thermal analysis parameters as inputs. A very good accordance between the measured and the predicted microstructure constituents was achieved. This allows for corrective measures to be taken with the purpose of obtaining the required microstructure and mechanical properties of castings as well as the decrease in the percentage of the waste castings.

REFERENCES

- [1] D. Venugopalan, Metallurgical Transactions A, **21**, 913-918 (1990).
- [2] X. Guo, D. M. Stefanescu, AFS Transactions **105**, 533-543 (1997).
- [3] E. N. Pan, W. S. Hsu, C. R. Loper, AFS Transactions **96**, 645-660 (1988).
- [4] D. Venugopalan, AFS Transactions **98**, 465-469 (1990).
- [5] T. Skaland, Ø Grong, AFS Transactions **99**, 153-157 (1991).
- [6] D. Venugopalan, A. Alagarsamy, AFS Transactions **98**, 395-400 (1990).
- [7] F. Unkić, F. Gavranović, N. Vasilić, M. Strojarsvo, **47**, 33-38, (2005).
- [8] P. Mrvar, Scandinavian Journal of Metallurgy **31**, 393-400 (2002).
- [9] P. Mrvar, Materials Science Forum **508**, 287-294 (2006).
- [10] R. W. Heine, AFS Transactions **101**, 879-884 (1993).
- [11] G. M. Goodrich, D. P. Jones, AFS Transactions **101**, 1031-1037 (1993).
- [12] D. M. Stefanescu, In: Proceedings of the Third International Symposium on the Physical Metallurgy of Cast Iron, Eds.: Fredriksson, H.; Hillert, M., Stockholm, Sweden, Materials Research Society, 151-162, (1984).
- [13] C. Labrecque, M. Gagné, AFS Transactions **106**, 83-90, (1998).
- [14] S. Chang, D. Shangguan, D. M. Stefanescu, AFS Transactions **99**, 531-541 (1991).
- [15] M. T. Hagan, H. B. Demuth, M. H. Beale, Neural Network Design, PWS Publishing Company, (1996).

Received: 10 January 2009.

